2015

Early Spring Phytoplankton Dynamics in the Subpolar North Atlantic: The Influence of Protistan Herbivory

Françoise Morison

Susanne Menden-Deuer
University of Rhode Island, smenden@uri.edu

Early spring phytoplankton dynamics in the subpolar North Atlantic: The influence of protistan herbivory

Françoise Morison* Susanne Menden-Deuer
Graduate School of Oceanography, University of Rhode Island, Narragansett, Rhode Island

Abstract

We measured phytoplankton-growth (μ) and herbivorous-protist grazing (g) rates in relation to mixed-layer-depth (MLD) during the March/April 2012 EuroBasin cruise in the subpolar North Atlantic. We performed 15 dilution experiments at two open-ocean ($\sim$ 1300 m) and one shelf (160 m) station. Of the two open-ocean stations one was deeply mixed (476 m), the other stratified (46 m). At the shelf station, MLD reached the bottom. Initial chlorophyll a (Chl a) varied from 0.2–1.9 μg L^{-1} and increased up to 2.7 μg L^{-1} at the shelf station. In 80% of experiments, regardless of MLD, growth-rates exceeded grazing-mortality rates. At the open-ocean stations, the deep ML coincided with μ and g that varied over the same range ($\leq$ 0–0.6 d^{-1}), whereas stratification corresponded to μ and g that ranged from 0.14–0.41 d^{-1} to 0.11–0.34 d^{-1}, respectively. At the stratified station, the balance between μ and g explained 98% of in situ variations in Chl a, whereas at the deep-ML station, rate estimates had no explanatory power. The consistent relationship between μ and g, which corresponded to a grazing-removal of 64% of primary production, suggests that g might be predictable if μ is known, and that a coefficient of 0.64 may be a useful parameter for subarctic carbon models. Composition and persistence of the plankton assemblages differed at the stations and may have been a significant driver of grazing-pressure. Overall, these results showed no association of MLD with grazing-pressure and highlight the need to assess to what extent MLD represents the depth of active-mixing to understand the effects of protistan-grazing on the development of the North Atlantic spring bloom.

In the subpolar North Atlantic, the yearly cycle of primary production (PP) is dominated by the annual recurrence of the spring phytoplankton bloom. The seasonal increase in phytoplankton biomass is of large biogeochemical significance, as the associated vertical export of fixed carbon (Turner 2002; Alkire et al. 2012) contributes to the large drawdown of atmospheric CO_2 that occurs in the North Atlantic (Takahashi et al. 2009).

For a bloom (i.e., an accumulation of biomass) to occur, net phytoplankton population growth rate (i.e., accumulation rate) needs to be positive, that is the phytoplankton instantaneous growth rate (μ), has to exceed the rate at which production is lost (Banse 1994). The accumulation rate thus results from the balance between the growth and loss terms. Yet, as recently pointed out (Behrenfeld and Boss 2014), in the extensive research of potential triggers of the North Atlantic spring bloom, only one of the two terms, the growth term (μ), has historically received most attention. In particular, a large

focus has been placed on the influence on μ of one physical variable: mixed layer depth (MLD); MLD is a proxy for, yet not always representative of, the actively mixing layer (Brainerd and Gregg 1995; Ferrari et al., in press; Franks, in press).

As early as 1935, Gran and Braarud (1935) developed the concept of a "critical depth," i.e., the depth of a mixed layer within which integrated phytoplankton production and losses are equal. Sverdrup (1953) formalized the idea that the North Atlantic spring bloom is initiated when the mixed layer shoals above the critical depth into a hypothesis that to this day continues to serve as a paradigm for the understanding of bloom formation (e.g., Siegel et al. 2002; Henson et al. 2006; Lindemann and St. John 2014). Yet in accordance with Sverdrup's own cautious remarks, numerous observations have been reported of early spring surface increases in phytoplankton biomass preceding stratification (e.g., Townsend et al. 1992, 1994; Dale et al. 1999), challenging a simplified model that makes stratification a prerequisite of bloom formation. Consequent new hypotheses have continued to focus on potential factors driving μ, all involving the extent of vertical mixing: for example, rates of turbulent mixing (Huisman et al. 1999, 2002), heat-flux induced weakening of turbulent mixing (Taylor and Ferrari 2011; Ferrari et al., in

press), and eddy-driven stratification (Mahadevan et al. 2012). Thus traditionally, in the determination of bloom formation mechanisms, a disproportionate emphasis has been placed on vertical mixing and its effects on μ, whereas the phytoplankton-mortality term has been much less studied.

Of all losses affecting PP, the quantitatively most significant is due to grazing (Banse 1994). In particular, the majority of ocean PP is consumed by ubiquitous $< 200 \ \mu m$ herbivorous protists (HP), a group dominated by ciliates and dinoflagellates (Smetacek 1981; Calbet and Landry 2004; Strom and Fredrickson 2008). Thanks to their diverse feeding strategies, protist grazers can access a range of prey sizes spanning from bacteria to chain-forming phytoplankton (Sherr and Sherr 2002; Sherr et al. 2013), resulting in a wide range of predator-prey size ratios. HP grow at rates similar to their prey, allowing predator numbers to often increase quickly after an increase in available prey (Sherr et al. 2003). From a plethora of studies performed in diverse marine habitats, HP grazing impact has been estimated to average $\sim$ 69% of PP (Calbet and Landry 2004). Although temporal and spatial exceptions exist, in which other loss processes such as viral lysis (Brussaard 2004), nutrient starvation (Taylor et al. 1993), and/or vertical export (Martin et al. 2011; Alkire et al. 2012) control phytoplankton biomass, HP herbivory has been established as the most significant loss factor in PP.

From the research that has considered the role of grazing losses in phytoplankton blooms, a consensus has emerged that seasonal high-latitude blooms happen because grazer-induced biomass removal cannot keep pace with phytoplankton growth. Various mechanisms have been proposed, including phytoplankton predation-avoidance strategies (Irigoien et al. 2005), physiological depression of growth rates that are thought to be greater for predators than for phytoplankton at temperatures $< 5°C$ (Rose and Caron 2007), low pre-bloom availability of prey (Sherr and Sherr 2009; Sherr et al. 2013), or unsuitability of available prey species (Gifford et al. 1995), all resulting in phytoplankton growth that exceeds grazing mortality.

Recent work by Behrenfeld and colleagues (Behrenfeld 2010, 2014; Behrenfeld et al. 2013; Behrenfeld and Boss 2014) has re-examined the importance of the physics of MLD to phytoplankton-bloom formation, by considering MLD's effects not only on phytoplankton growth as has been traditionally done but also on the magnitude of grazing pressure. Behrenfeld (2010) suggested that a key process influencing variations in the North Atlantic phytoplankton biomass is the degree to which vertical mixing alters the balance between μ and g. Using satellite-derived estimates of phytoplankton-biomass accumulation rates as a function of MLD, Behrenfeld (2010) demonstrated that the spring bloom "initiates," i.e., phytoplankton accumulation rate first becomes positive, not when ML shoals but during winter when ML deepens.

Bloom initiation is therefore observed when the biomass accumulation rate becomes positive although quantitatively minuscule, and differs from other definitions of what constitutes a bloom. Many definitions are based on bulk properties such as when chlorophyll levels (a proxy for phytoplankton biomass) exceed some threshold concentration, or on when the accumulation rate is largest (e.g., Sherr and Sherr 2009; Brody et al. 2013), although some of these criteria have been argued to short-change our full understanding of bloom formation (Smayda 1997).

According to the Disturbance-Recovery Hypothesis (DRH) (Behrenfeld et al. 2013; Behrenfeld 2014; Behrenfeld and Boss 2014), which evolved from the earlier Dilution-Recoupling hypothesis (Behrenfeld 2010), blooms start when a process disturbs the balance between phytoplankton growth and predation mortality: in the subpolar North Atlantic, this "disturbance" is caused by deepening of the mixed layer. Dilution by entrainment of deep particle-free water reduces density-driven grazing rates by lowering encounters between predators and their diminishing prey. This process eventually allows low winter phytoplankton division rates to exceed grazing losses and thus the "blooming phase" to initiate (i.e., the accumulation rate to become positive). Sustained dilution by deepening of the mixed layer, however, prevents a rise in phytoplankton concentration. The "recovery" stage of the DRH begins when mixed layer deepening stops, allowing a volumetric increase in phytoplankton. Although at this time predators' and prey concentrations rise in parallel, the light-driven, slow but steady acceleration in division rates maintains a positive accumulation rate that leads to the bloom climax. Increased prey density and physical recoupling between predators and prey via stratification results in overgrazing, which along with decreasing division rates contributes to the "declining phase" of phytoplankton biomass.

While data from both satellite (Behrenfeld 2010) and profiling floats (Boss and Behrenfeld 2010) provided strong evidence of wintertime deep mixed layers corresponding to small but positive phytoplankton biomass accumulation rates, the mechanism driving the annual cycle of phytoplankton biomass hypothesized by Behrenfeld (2014) has not been tested in the field. In the open North Atlantic ocean at high latitudes above 50°N, where winter MLD is typically large due to convection (Backhaus et al. 2003), existing bloom-related in situ measurements of HP grazing rates come from studies conducted during (Gifford et al. 1995; Stelfox-Widdicombe et al. 2000; Gaul and Antia 2001) or after the phytoplankton spring bloom biomass maxima (Burkill et al. 1993; Gifford et al. 1995). In particular, to our best knowledge there are no empirical data of grazing rates for the critical period during which phytoplankton biomass increases from winter concentration to the bloom climax.

Here we evaluate the importance of grazing mortality in the dynamics of phytoplankton biomass during this transitional period. We present results of measurements of HP grazing and phytoplankton growth rates performed from 26

Table 1. Characteristics of source water used in dilution experiments (T = water temperature, MLD = mixed layer depth, Z_{eu} = euphotic depth). "Dark" represents a night CTD cast.

Date	CTD cast #	Water collection depth (m)	T in situ (°C)	Salinity (PSU)	MLD (m)	Z_{eu} (m)
Station 1 (Iceland Basin − Total depth = 1345 m)						
26 Mar	424-1	30	8.7	35.30	601	108
09 Apr	523-1	30	8.6	35.29	524	64
10 Apr	541-1	18	8.6	35.30	452	65
18 Apr	611-1	40	8.7	35.29	551	47
19 Apr	624-1	35	8.6	35.28	642	63
28 Apr	679-1	25	8.6	35.28	498	79
Station 2 (Norwegian Basin − Total depth = 1298 m)						
31 Mar	460-1	20	7.1	35.19	48	Dark
31 Mar*	460-1	20	7.1	35.19	48	Dark
13 Apr	564-1	35	6.4	35.14	30	62
14 Apr	578-1	30	6.6	35.15	36	65
14 Apr*	578-1	5	6.8	35.18	36	65
23 Apr	649-1	20	6.8	35.18	29	64
24 Apr	659-1	35	7.0	35.19	68	53
Station 3 (Norwegian Shelf − Total depth = 163 m)						
02 Apr	487-1	30	7.8	35.36	Bottom (160 m)	63
16 Apr	605-1	30	7.8	35.37	Bottom (160 m)	52

*Experiment conducted at surface (instead of depth adjusted) irradiance.

March 2012 to 28 April 2012, during the EuroBasin program "Deep Convection" cruise to three study sites in the subpolar North Atlantic. We sampled at one shelf and two open-ocean stations, which contrasted in MLD. We found that in early spring, phytoplankton growth rates largely exceeded grazer-induced losses and that MLD was a poor predictor of both the magnitude of grazing rates and the potential for biomass accumulation.

Methods

Sampling sites and in situ environmental conditions

Protistan herbivory was quantified during 2–4 visits at each of two ~1300–m deep open-ocean sites located in the Iceland Basin (S1) and the Norwegian Sea (S2), and at a ~160–m deep site located on the Shetland shelf (S3) (Table 1).

We used hydrological data collected by a SBE911Plus Sea-bird Electronics CTD equipped with a WET Lab ECO-FLNTU(RT)D chlorophyll sensor to characterize in situ conditions at the depth of sample collection, as well as general environmental conditions encountered during the study. A total of 20, 14, and 9 full-depth CTD casts were available for S1, S2, and S3 respectively, which we used to generate estimates of mixed-layer depth (MLD), average mixed-layer temperature (T) and salinity, and MLD integrated chlorophyll *a* (Chl *a*). To define MLD, we used a potential-T threshold criterion of −0.2°C from a reference depth of 10 m (de Boyer Montégut et al. 2004).

Using PAR data obtained from a biospherical QSP-2350L Quantum Scalar PAR sensor mounted on the CTD, we estimated the euphotic depth (Z_{eu} = depth receiving 1% of surface irradiance; Falkowski and Raven 2007; Behrenfeld 2010) from the regression coefficient of the natural log of PAR values vs. depth, which corresponds to the coefficient of vertical light extinction (Falkowski and Raven 2007).

Protistan herbivory

We measured HP grazing rates in 15 separate experiments using the Landry and Hasset (1982) dilution method. Water containing the plankton assemblage for the experiments was collected using Niskin bottles mounted on the CTD rosette sampler. Depth of water collection corresponded to the CTD fluorescence maximum (F_{max}), except at S2 on March 31st (no F_{max}) and on April 14th when two depths were sampled (F_{max} and 5 m; Table 1). We used F_{max} as a proxy for maximum biomass and chose it as the collection depth to ensure that biomass in the dilution experiments was sufficient for an appropriate signal-to-noise ratio and a detectable change in Chl *a* even in the most dilute incubations. Water was gently transferred from the Niskin bottles into 10-L carboys via a silicone tube, to which a 200-μm mesh was affixed in order to screen out larger grazers. We refer to this < 200-μm fraction as whole seawater (WSW).

The dilution method involves setting up a series of dilution treatments (usually 4–5) to create a gradient in grazers'

abundance. Although we followed this experimental set up, we present phytoplankton growth and grazing mortality rates estimated following the two-point method (Worden and Binder 2003), using only the lowest dilution and the undiluted treatments (see Phytoplankton growth and grazing mortality rates below).

Filtered seawater (FSW) used to dilute the plankton assemblage was obtained by gravity-filtration of water collected from the same site and depth through a 0.2-μm capsule filter (Pall). For the diluted treatment used in determining rates, the combination of WSW and FSW resulted in a dilution factor that averaged 8% $\pm$ 2% WSW. To avoid variation among replicates, the diluted treatment was prepared in a single carboy as a large volume stock and was then gently siphoned into the incubation bottles. Both the diluted and undiluted treatments were incubated in duplicate 2.4-L polycarbonate bottles. To ensure sufficient nutrients for phytoplankton growth (Landry and Hasset 1982) all bottles were amended with final concentrations of 8.82 μM nitrate, 0.48 μM phosphate, and 10 μM silicate. To check for effects of nutrient addition and for nutrient limitation, additional WSW replicates were incubated without added nutrients.

Bottles were incubated for 24 h. All incubations took place in on-deck 250-L tanks. Bottles were suspended midwater by strapping them onto bungee cords loosely stretched across the length of the tanks, which together with ship motion provided gentle agitation. Incubations were maintained at in situ surface temperature by flow-through of ambient seawater. Incubation temperature was recorded at 30-mn intervals using in-tank Hobo data loggers. Incubation temperature was on average 0.9 ($\pm$ 1.1)°C higher than the temperature at collection depth, however departures from mean temperature occurred mainly during the 1st leg of the cruise, when differences were the largest during the 1st experiments at S2 and S3. For the remainder, differences between in situ and incubator temperatures averaged 0.5 ($\pm$0.5)°C.

To minimize chlorophyll bleaching, which is known to occur in light-sensitive polar phytoplankton (Smith and Sakshaug 1990; Caron et al. 2000), bottles were incubated in black neutral-density mesh-bags that reduced the light to 30% of surface irradiance. Incubations carried at collection-depth irradiance fail to truly replicate the average light regime experienced by cells in a mixed layer (Ross et al. 2011), therefore, the same mesh screen was generally used regardless of water collection-depth. There were two exceptions: (1) no mesh screen was used in the April 14th incubation from 5 m; (2) to investigate the effect of light on rate magnitudes, on March 31st, a set of two experiments were incubated simultaneously, one with and one without screen.

Phytoplankton growth and grazing mortality rates

Phytoplankton growth and HP grazing mortality rates were estimated from changes in extracted Chl a (Landry and Hasset 1982). Initial and final Chl a concentrations were determined from triplicate subsamples of each initial stock and of each replicate bottle respectively. Subsamples ranged in volume from 60 mL to 500 mL depending on the in situ Chl a concentration and the dilution level. Chl a extraction and determination followed Graff and Rynearson (2011), except that extraction took place at room temperature for 12–15 h in 96% ethanol (Jespersen and Christoffersen 1987).

Apparent phytoplankton growth rate (k, d^{-1}) in each bottle was estimated using the equation $k = 1/t \ln (P_t - P_0)$, where t = incubation time in days, and P_t and P_0 are respectively the final and the initial Chl a concentrations. Following the dilution method (Landry and Hasset 1982), the instantaneous phytoplankton growth rate μ (d^{-1}) and the instantaneous grazing rate g (d^{-1}) are determined from the coefficients of a linear regression analysis of k in the various dilution treatments vs. their respective dilution factor. The regression coefficients, y-intercept and negative slope, represent μ and g respectively. Hence one of the dilution method's major assumptions is that k be a linear function of the dilution factor. When testing whether the linearity assumption held for all dilution experiments, we found significant deviations from linearity in four experiments (data not shown). Therefore, for all experiments we estimated μ and g using Worden and Binder's (2003) two-point method. In this method, the grazing rate is calculated as the difference between the apparent phytoplankton growth rate (k) in the lowest and highest fractions of WSW; k in the most dilute treatment serves as an estimate of μ. Rate estimates obtained using the two-point approach are considered conservative (Worden and Binder 2003; Lawrence and Menden-Deuer 2012) and in general do not vary significantly from rates obtained using a linear regression (Worden and Binder 2003; Strom and Fredrickson 2008; Morison and Menden-Deuer, unpubl.). We found no significant difference between k in undiluted treatments with and without nutrients ($p = 0.63$, 0.21, and 0.15 for S1, S2, and S3, respectively). Consequently we assumed in situ nutrients were in excess, and used the average k value of all undiluted replicates when calculating grazing rates. The grazing impact of HP in terms of the proportion of primary production (PP) consumed was calculated as % PP = g : $\mu \times 100$ following Calbet and Landry (2004). For all calculations, negative growth rate and negative grazing rate estimates were corrected to +0.01 d^{-1} and zero respectively (Calbet and Landry 2004). Grazing impact (% PP) was not calculated for experiments in which no significant phytoplankton growth was measured. To provide integrated averages across conditions zero values were included in the calculation of averages.

To assess to what degree the balance between phytoplankton growth and grazing losses determined the in situ dynamics of phytoplankton biomass, using Chl a as a proxy for biomass, we compared observed (i.e., in situ) Chl a accumulation rates (r_{obs}) to the accumulation rates inferred from experimentally determined phytoplankton growth and mortality rates ($r_{calc} = \mu - g$). The observed accumulation rate was

determined using the equation $r_{obs} = 1/t \times \ln(P_t - P_0)$ where P_t and P_0 are final and initial Chl a concentrations over the time interval (t) separating two consecutive experiments at the same station.

Plankton biomass and species composition

To determine plankton biomass and species composition, well-mixed subsamples of the initial undiluted treatments of each experiment were preserved with acidified Lugol's iodine at a final concentration of 2% (Menden-Deuer et al. 2001). Diatoms, dinoflagellates, and ciliates were enumerated by settling 50 mL for a minimum of 24 h following the Utermöhl (1958) method. Since enumeration of heterotrophic nanoflagellates using the Utermöhl method results in underestimates (Davis and Sieburth 1982), these organisms were not counted, although they can be abundant and active grazers (Verity et al. 1999; Stelfox-Widdicombe et al. 2000) and likely do contribute to the grazing rates measured here. Among the groups that we enumerated, only diatoms are considered strict non-phagotrophs (Flynn et al. 2013). Although most dinoflagellates and ciliates function as mixotrophs (Flynn et al. 2013), because of their phagotrophic capacity, they were categorized as herbivorous, except for the obligate mixotroph ciliate *Mesodinium rubrum* (Hansen et al. 2012), which was not included in the herbivorous biomass and abundance estimates.

Diatoms were identified to genus following Throndsen et al. (2007) and Kraberg et al. (2010). Dinoflagellates were divided into thecate and athecate groups, and when possible further identified to genus following Dodge (1982), or assigned to a morphotype (based on similarity of shape). Enumerated ciliates were divided into loricate (tintinnids) and aloricate groups. To provide a qualitative description of the ciliate community, higher taxonomic identification of aloricate ciliates relying on shape was made following Strüder-Kypke et al. (2002), but due to its limited reliability (Montagnes and Lynn 1991), these higher-level identifications were not used for quantitative analysis. Linear cell dimensions were measured using ImageJ software (National Institute of Health) from images taken of all dinoflagellates and ciliates contained in each sample and, depending on abundance, of all or a subset of diatom cells (30–300 cells per genus). Cell volumes were calculated from linear dimensions using appropriate geometric shape algorithms. Biomass estimates were calculated by converting biovolumes into carbon content (μg C L^{-1}) applying the following conversion factors: tintinnid ciliates, Verity and Langdon (1984); aloricate ciliates, Putt and Stoecker (1989); all other plankton groups, Menden-Deuer and Lessard (2000).

Statistical analyses

A correlation-based principal component analysis (PCA) was used to characterize environmental variability. Included in the analysis were log-transformed data from CTD casts used to collect water for the experiments of in situ temperature and salinity, and estimates of MLD, and Z_{eu}.

Patterns in the composition of the diatom and of the HP assemblages were investigated using the nonparametric multivariate statistics package Primer-E (Plymouth Routines in Multivariate Ecological Research, version 6; Clarke and Gorley 2006). To visualize multivariate patterns, multidimensional scaling (MDS) and cluster analyses (Clarke 1993) were performed on Bray–Curtis index-based similarity matrices. The similarity matrices were obtained using biomass data that were 4th root transformed to even out contribution among groups. Points close together represent samples that are similar in species composition. Stress values indicate how well the two-dimensional plot summarizes the rank-order relationships between samples. Values of stress < 0.1 are considered to correspond to a good ordination and values < 0.2 provide a less satisfactory but still useful assessment of the degree of relatedness among samples (Clarke 1993).

To further assess the nature and strength of relationships among plankton samples, an analysis of similarity (ANOSIM) was performed on the resemblance matrices. ANOSIM is a nonparametric permutation procedure that computes the global R statistic, which can range from -1 to 1, although negative values are unlikely (Clarke and Warwick 2001). Values approaching 1 indicate greater similarities within a group than among groups, whereas values approaching zero indicate no group associations/clustering.

The RELATE Primer-E statistical routine was performed using Spearman rank correlation to explore correlations between biotic and environmental patterns. Plankton biomass-based similarity matrices were also used to compare plankton assemblages using station and grazing magnitude as separate factors. Grazing pressure was partitioned into three levels relative to the overall average (zero, below average, and above average). To examine if species composition influenced whether grazing occurred at all, the analysis was repeated using only two levels distinguishing measurable from nonmeasurable grazing.

The effect of nutrient addition was evaluated using a two-tailed paired t-test to compare measurements of apparent phytoplankton growth (k) in amended and nonamended undiluted treatments. Linear regressions were tested for deviations from linearity using ANOVA (Zar 2010).

Finally, a series of univariate analyses (linear regression and Pearson correlation) were performed using SigmaPlot® software to examine relationships between grazing rates and a series of potential driving factors. All statistical analyses were performed at an alpha level of 0.05. All rates and other estimates are expressed $\pm$ one standard deviation of the mean.
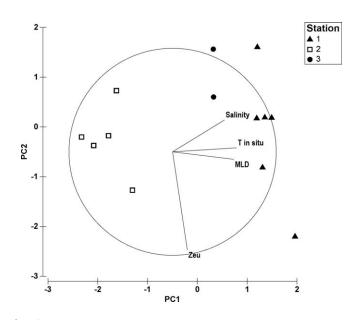
Results

In situ conditions

The three stations were well distinguished by persistent contrasting environmental conditions. Data from all CTD casts (not shown) performed over the entire duration of the

cruise provided evidence that the spatial variation in physical parameters among stations was greater than temporal variation within stations. Stations significantly differed in MLD (ANOVA, $p < 0.001$). S1 had a deep ML that averaged 476 ± 149 m. MLD at S2 was one order of magnitude shallower than at S1, averaging 46 ± 16 m. At the shallow (160 m) shelf station S3, MLD always reached the bottom. Consequently, MLD at S1 was deeper and MLD at S2 was generally shallower than the average euphotic depth (70 ± 18 m and 70 ± 10 m at S1 and S2, respectively) estimated from all daytime CTD casts ($n = 13$ and 9). On the shelf at S3, MLD was always deeper than the mean euphotic depth (50 ± 11 m, $n = 6$). Stations also differed in T and salinity. Mixed-layer average T was warmest at S1, where over the sampling period, it averaged 8.6 ($\pm$ 0.23)°C, and T was coldest at S2 where it averaged 6.9 ($\pm$ 0.24)°C. At S3, T averaged 7.8 ($\pm$ 0.15)°C. Differences in mixed-layer average salinity among stations were small yet distinctive, averaging 35.28 ($\pm$ 0.04), 35.18 ($\pm$ 0.02), and 35.36 ($\pm$ 0.01) at S1, S2, and S3 respectively. T, MLD, and salinity were the primary drivers of the differences in ambient environmental conditions among the three stations (Table 1), which were significant (ANOSIM global $R = 0.796$, $p = 0.002$; Fig. 1). Together the first two axes of the PCA explained 89.6% of the variance of the in situ data.

Rate estimates

Initial < 200 μm Chl a levels during our experiments ranged from 0.17 μg L^{-1} at S1 to 2.65 μg L^{-1} at S3, and averaged 1.02 ($\pm$ 0.54), 0.71 ($\pm$ 0.22), and 1.60 ($\pm$ 1.49) μg L^{-1} at S1, S2, and S3 respectively (Table 2). Over the entire sampling period and across all stations, phytoplankton growth rates ranged from -0.06 d^{-1} to 0.63 d^{-1} and mortality rates due to HP grazing ranged from 0 d^{-1} to 0.56 d^{-1} (Table 2).

In all but three measurements, phytoplankton growth rates exceeded grazing mortality rates (Fig. 2). The magnitude and variability of growth and grazing rates at S1 and S2 differed, with S1 exhibiting both higher rates and higher variability. At S1 growth and grazing rates varied over the same range (0–0.6 d^{-1}), and average growth rate 0.35 d^{-1} ($\pm$ 0.03) exceeded average grazing rate 0.25 ($\pm$ 0.04) d^{-1} (Table 2). There was one exception to the general decoupling between growth and grazing rates at S1: on 10 April, rates were highly coupled (0.60 d^{-1} and 0.56 d^{-1} respectively), and corresponded to the highest initial concentration of Chl a (1.9 μg L^{-1}) at that station (Table 2).

At S2, growth rates ranged from 0.18 d^{-1} to 0.41 d^{-1} and grazing rates ranged from 0.11 d^{-1} to 0.34 d^{-1}. Growth and grazing rates had similar averages (0.24 $\pm$ 0.02 d^{-1} and 0.22 $\pm$ 0.03 d^{-1}, respectively) (Table 2). On the last two sampling dates, the balance between phytoplankton growth and grazing rates changed from positive to negative. When water from the same source was incubated at two different irradi-

Fig. 1. Principal component analysis (PCA) ordination of in situ conditions at stations 1 (▲), 2 (□), and 3 (•). PC1 and PC2 together account for 89.6% of the variation. PC1 (eigenvalue = 2.49) represents an axis of decreasing in situ temperature (T) and MLD, each variable having a similar eigenvector coefficient (0.618 for T and 0.590 for MLD). Euphotic depth (Z_{eu}) was the major contributor (eigenvector coefficient = -0.948) to PC2 (eigenvalue = 1.11) and varied more within than across stations. Samples belonging to the same station tended to segregate along the MLD and T gradient. Grouping was significant (ANOSIM global $R = 0.796$ $p = 0.0002$, 999 permutations).

ance levels (31st March), the higher light regime reduced phytoplankton growth rate by 35%, whereas grazing rates were unaffected (Table 2). When experimental water was collected from two different depths (5 m and 30 m), phytoplankton growth rate was 70% lower at the 5-m depth compared to 30-m, despite similar initial Chl a concentration. Grazing rate on the other hand was approx. twice higher at 5-m depth (Table 2) despite a similar HP biomass.
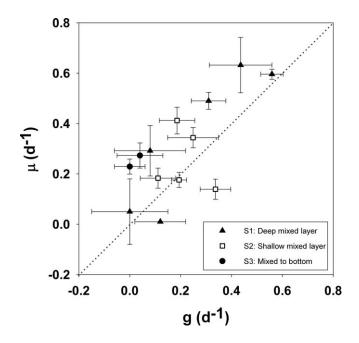
On the Norwegian shelf (S3), only two experiments were performed at a 2-week interval. The first experiment yielded no detectable grazing, and a very low grazing rate (0.04 d^{-1}) was measured the second time (Table 2), whereas phytoplankton growth rates were similar on both dates (0.23 d^{-1} and 0.27 d^{-1}).

Grazing magnitude was independent of MLD (Fig. 3). Results of a series of univariate analyses indicated no significant correlations of either μ or g with any of the ancillary variables, including collection depth. Nor was there any correlation with initial phytoplankton biomass (Chl a). HP species assemblages did not significantly vary according to grazing pressure (absence or presence of grazing) or category of grazing magnitude (below average, average, above average), suggesting that taken separately, the species composition of either the prey or the predator assemblage did not directly influence phytoplankton grazing-mortality.
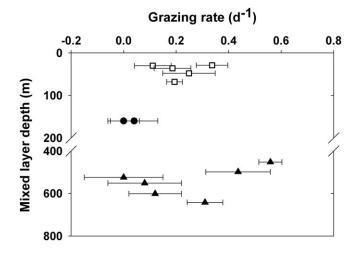
Table 2. Initial Chl *a* concentration (μg L^{-1}), phytoplankton growth (μ, d^{-1}) and grazing mortality (*g*, d^{-1}) rates, and grazing impact as % of primary production (% PP) consumed. Values in parentheses represent 1 standard deviation of the mean.

Date	Chl *a*	μ	*g*	% PP
Station 1				
26 Mar	0.17 (0.01)	−0.06* (0.001)	0.12 (0.10)	n/a
09 Apr	0.99 (0.01)	0.05 (0.13)	−0.10* (0.15)	0
10 Apr	1.87 (0.03)	0.60 (0.02)	0.56 (0.08)	94
18 Apr	1.13 (0.04)	0.29 (0.10)	0.08 (0.14)	26
19 Apr	0.96 (0.03)	0.49 (0.03)	0.31 (0.07)	63
28 Apr	1.02 (0.02)	0.63 (0.11)	0.44 (0.12)	69
Average	1.02	0.35	0.25	50
Station 2				
31 Mar	0.49 (0.02)	0.34 (0.04)	0.25 (0.10)	72
13 Apr	0.60 (0.01)	0.18 (0.04)	0.11 (0.06)	61
14 Apr	0.59 (0.03)	0.41 (0.05)	0.19 (0.07)	45
23 Apr	1.03 (0.03)	0.14 (0.04)	0.34 (0.06)	242
24 Apr	0.85 (0.02)	0.18 (0.03)	0.19 (0.03)	110
Average	0.71	0.25	0.22	106
Experiments incubated at surface irradiance				
31 Mar	0.49 (0.02)	0.25 (0.04)	0.26 (0.06)	104
14 Apr	0.64 (0.10)	0.12 (0.03)	0.32 (0.06)	267
Station 3				
02 Apr	0.54 (0.04)	0.23 (0.03)	−0.03* (0.06)	0
16 Apr	2.65 (0.05)	0.27 (0.05)	0.04 (0.09)	15
Average	1.60	0.25	0.02	8

*See text for treatment of negative values of μ and *g*.

Fig. 2. Phytoplankton growth rates vs. herbivorous protist grazing rates at S1 (▲), S2 (□), and S3 (•). Dashed line represents 1 : 1 ratio. Error bars represent one standard deviation of the mean.

Fig. 3. Herbivorous Protist grazing rates (d^{-1}) as a function of MLD (m). Symbols correspond to stations, as specified in Fig. 2 legend.

Grazing impact on primary production

Despite positive grazing rates being generally higher at S1 than at S2, the grazing impact was on average highest at S2 (Table 2). At S1 PP consumed averaged 50 (± 37)%, varying from 0% to 94%. At S2 PP consumed varied between 45% and 242% (Table 2). At S2, the average PP consumed was 59% until mid-April, and increased to an average of 176% on the last visit to the station, equivalent to an overall average of 106 (± 80)% (Table 2). At S3, the average PP consumed was 8%.
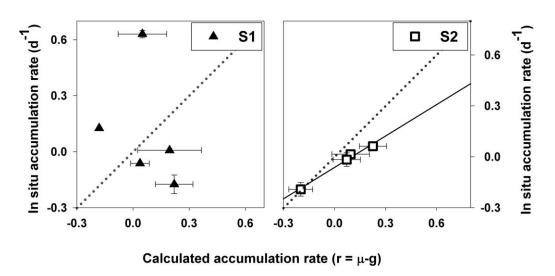
While grazing impact was variable, an overall relationship between phytoplankton growth and grazing mortality existed that could be expressed in terms of the linear regression equation

$$g = 0.642\,\mu + 0.014$$

The regression coefficient corresponds to a grazer-induced removal of 64% of PP ($R^2 = 0.526$, $p = 0.005$, SE = 0.18). When only experiments in which $\mu > g$ are considered (Fig. 2), $g = 0.946 - 0.13$ ($R^2 = 0.83$, $p = 0.0002$, SE = 0.15).

Influence of grazing on dynamics of phytoplankton biomass

The oceanic stations differed in the level to which in situ Chl *a* variations followed the dynamics inferred from the rate measurements made with the dilution method. At S1, changes in Chl *a* did not match those inferred by the rate estimates ($R^2 = 0.10$, $p = 0.61$) (Fig. 4a). In contrast at S2, the measured variation in Chl *a* closely matched the balance between experimentally estimated rates ($R^2 = 0.98$, $p = 0.009$) (Fig. 4b). In the dilution experiments performed at S1, we measured a tenfold increase in Chl *a* concentration, from 0.2 μg L^{-1} to 1.9 μg L^{-1} between 26 March and 10 April, which clearly exceeded the ~ zero growth rates measured in the
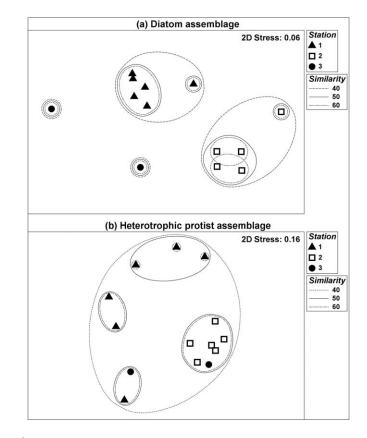
Fig. 4. Daily net calculated ($\mu - g$; x-axis) vs. net in situ phytoplankton accumulation rates (y-axis), the latter estimated from changes in in situ Chl *a* concentration measured at the beginning of each experiment, for the two oceanic stations: regression of *x* vs. *y* variables yielded (a) S1 ($R^2 = 0.10$, $p = 0.60$), (b) S2 ($R^2 = 0.98$, $p = 0.009$). The significant regression for S2 is shown on the graph. Dashed lines represent the 1 : 1 ratio. Apparent lack of error bars means that due to their small values, error bars are obscured by symbol.

dilution experiments over the same period. For the remainder of the sampling period, Chl *a* remained $\sim 1\ \mu g\ L^{-1}$, despite the fact that phytoplankton growth rates exceeded grazing rates. Based on CTD data, MLD-integrated Chl *a* concentration increased from $\sim 40\ mg\ m^{-2}$ at the 1st visit to 230–250 mg m^{-2} during visits 3 and 4, and up to 75% of this increase occurred below the euphotic zone.

At S3, based on estimated rates and assuming no other losses than grazing, the phytoplankton abundance would have doubled every ~ 3 d, twice more often than indicated by the increase in Chl *a* from 0.5 $\mu g\ L^{-1}$ to 2.7 $\mu g\ L^{-1}$ over 2 weeks.

Composition of the plankton community biomass

There were clear differences between the composition of the plankton biomass of S1 and S2 (Fig. 5). Both the diatom (Fig. 5a) and the HP assemblages (Fig. 5b) were strongly associated with location (ANOSIM $p \leq 0.002$), and plankton communities from S1 and S2 differed the most ($p = 0.002$). Temporal variability of HP assemblage was greater among samples from S1 than among samples from S2, whereas the reverse was true for diatoms, which at S2 were scarce (see below). Lowest similarity between experiments was observed at S3 for both the diatom ($<40\%$ similarity) and the HP assemblages ($<50\%$ similarity; Fig. 5). Diatom and HP assemblages both correlated with the multivariate pattern of environmental data characterized by the PCA (Primer-E statistical routine RELATE, Spearman correlation= 0.518 and 0.47, respectively, $p = 0.002$), confounding the ability to distinguish the relative influence of species composition and environmental conditions on grazing magnitude.

Fig. 5. Multidimensional scaling (MDS) analysis of species composition of (a) the diatom fraction of the autotrophic community and (b) herbivorous protists assemblage at stations 1 (▲), station 2 (□) and station 3 (•). Overlaid contours represent among-samples similarity levels of 40%, 50%, and 60% (CLUSTER analysis). Note that very few diatoms were present in samples at S2.

Table 3. Biomass estimates (μg carbon L^{-1}) of herbivorous protists (HP, dinoflagellates and ciliates only) and of diatoms contained in < 200 μm undiluted samples collected from the fluorescence maximum at the beginning of each dilution experiment. Biomass of aloricate ciliates, tintinnids, and dinoflagellates are given as a percentage of total HP biomass.

Date	HP	% Aloricate ciliates	% Tintinnid ciliates	% Dino- flagellates	Diatoms
Station 1					
26 Mar	1.2	82.9	0.8	16.3	0.32
09 Apr	2.0	44.7	21.1	34.2	7.54
10 Apr	2.4	42.6	0.0	57.4	15.89
18 Apr	3.2	45.7	13.3	41.0	8.27
19 Apr	4.9	33.6	15.8	50.6	5.73
28 Apr	2.8	74.7	0.0	25.3	6.05
Station 2					
31 Mar	4.6	92.1	0.0	7.9	0.06
13 Apr	2.6	88.0	0.9	11.1	0.04
14 Apr	7.9	94.3	0.0	5.7	0.07
23 Apr	10.4	79.8	1.9	18.2	0.20
24 Apr	6.1	82.6	2.1	15.2	0.04
Station 3					
02 Apr	1.8	76.3	0.0	23.7	0.56
16 Apr	6.1	86.6	7.0	6.4	87.69

Size structure and species composition of phytoplankton biomass

The dominant size fraction of the autotrophic community at each station differed. At S1, except for the 1st visit when autotrophic biomass was low and dominated by picoplankton, the > 50 μm Chl *a* fraction was composed of diatoms and contributed up to $\sim$ 50% of total Chl *a* (Paulsen et al., in review) Diatom biomass in samples, fluctuated between 0.3 μg C L^{-1} and 16 μg C L^{-1}, reaching maximum biomass on 10 April and decreasing thereafter (Table 3). In contrast at S2, diatoms were quasi-absent (average biomass < 0.1 μg C L^{-1}), and the > 10-μm Chl a fraction never exceeded 8% of total Chl *a* (Paulsen et al., in review). Between the two visits at S3, diatoms increased in biomass from 0.56 μg C L^{-1} to 87.7 μg C L^{-1} (Table 3).

Species and size distribution of herbivorous-protist biomass

HP assemblages differed among stations, both in species composition and biomass (Fig. 5). S1 HP assemblages were comprised of both ciliates and dinoflagellates, whereas S2 HP community was largely made up of ciliates. At S3 ciliates dominated the HP assemblage but there was a shift from small to large ciliates between the two sampling dates. Total HP biomass varied from 1.2 μg C L^{-1} (S1) to 10.4 μg C L^{-1} (S2), and averaged 2.8 ± 1.3 μg C L^{-1}, 6.4 ± 2.9 μg C L^{-1}, and 4 ± 3.1 μg C L^{-1} at S1, S2, and S3, respectively (Table 3).

At the three stations, aloricate ciliate biomass represented an average of $54\% \pm 20\%$, $88\% \pm 6\%$, $82\% \pm 7\%$ of the total herbivorous protist biomass. Aloricate ciliates included strobilidiid species of the genera *Lohmanniella* and *Leegaardiella*, as well as species of the genus *Strombidium*. The majority (45–100% biomass) of aloricate ciliates were 20–35 μm. At S1 there was an increase in the proportion of the > 50 μm ciliate size fraction from 0% to 47% of total aloricate ciliate biomass, whereas such large ciliates were absent from S2. At the 2nd visit at S3, 71% of aloricate ciliate biomass was made up of organisms > 50 μm. Only four tintinnid ciliate genera (*Acanthostomella* sp., *Parafavella* sp., *Salpingella* sp., and *Stenosomella* sp.) were observed across stations, always in low numbers.

Dinoflagellate types differed with station. At S1, on all dates except for the 1st visit, 50–100% of dinoflagellates were athecate gymnodinoid species. When thecate dinoflagellates were present, *Protoperidinium* spp. made up an average of 43 ($\pm$ 39)% of their biomass. At S2, an average of 48 ($\pm$ 17)% of dinoflagellate biomass was made up of small unidentifiable thecate forms. These small forms also dominated among dinoflagellates at the first visit at S3, when the < 10-μm size-fraction dominated total Chl *a*. Size distribution of dinoflagellates varied among experiments, but at S1, dinoflagellates > 50 μm represented $\sim$ 50% of all dinoflagellate biomass on the three dates coinciding with experiments that yielded the three highest grazing rates. Such large dinoflagellates were never observed at S2.

There was no within-station correlation between herbivorous biomass and Chl *a* concentration (Pearson correlation, S1 and S2 $p = 0.83$). One concern was that collection depth, which was determined by the fluorescence max and differed among experiments, might have affected concentration of protistan grazers and by extension grazing rates, but collection depth did not significantly influence either protistan grazers' numerical abundance ($p \geq 0.45$) or biomass ($p \geq 0.43$).

Discussion

Our study is, to our best knowledge, the first among a plethora of published field measurements (*see* Calbet and Landry 2004) to provide estimates of herbivorous protist grazing rates in the subpolar North Atlantic prior to the spring bloom climax. Such estimates are rare for this critical transition period, yet are much needed to test proposed hypotheses (e.g., Sherr and Sherr 2009; Behrenfeld 2010, 2014) about the role of HP feeding in the development of high latitude phytoplankton blooms. We also examined how MLD may have modulated the balance between μ and g, a process that has been suggested as a major factor controlling

Table 4. Grazing rates (*g*), proportion of primary production consumed (% PP), Chl *a* concentrations, and numerical abundance (10^3 cells L^{-1}) and biomass (μg C L^{-1}) of herbivorous protist grazers (HP) in studies previously conducted in the North Atlantic at similar latitudes as the present study during or after the phytoplankton spring bloom climax. Results from the present study are summarized for comparison.

Study	Month	Lat-Long	Chl *a* (μg L^{-1})	*g* (d^{-1})	% PP	HP abundance	HP biomass
Gifford et al. (1995)	May	59N–21W	0.59-2.89	0-1.01	56-64	3.3-6.9	n/a
Wolfe et al. (2000)	May	56N–45W	1.7	0.12	150	n/a	n/a
Burkill et al. (1993)	Jun	60N–20W	0.97	0.32	39	n/a	∼ 3.9
Stelfox-Widdicombe et al. (2000)	Jun	59N–20W	0.61-1.26	0.89-1.48	74	12.5-18.5	4.5-12.5
Gaul and Antia (2001)	Jul	62N–11W	0.79-1.15	0.52	55	n/a	5.2-6.5
This study (S1)	Mar–Apr	61N–11W	0.17-1.87	0-0.56	0-94	0.4-2.0	1.2-4.9
This study (S2)	Mar–Apr	63N–02W	0.49-1.03	0.11-0.34	45-242	3.4-12.0	2.6-10.3
This study (S3)	Mar–Apr	60N–01E	0.54-2.65	0-0.04	0-15	1.4-2	1.8-6.1

variations in phytoplankton biomass, including when the spring bloom initiates (Behrenfeld 2010, 2014).

In 80% of the experiments, the measured phytoplankton growth rates exceeded measured grazing rates. This result has two important ramifications. First, the positive phytoplankton biomass accumulation rates inferred from our estimates of μ and g imply an actively growing phytoplankton community for which biomass accumulation is not prevented by grazer-induced mortality losses. Second, although not tested in a formal experiment, our results do not fully support the inverse relationship between grazing pressure and MLD that one might expect based on the Disturbance Recovery Hypothesis (DRH) (Behrenfeld 2014).

The second ramification deserves some clarification. The DRH clearly emphasizes the importance of mixed-layer *deepening* (as distinguished from absolute magnitude of MLD) acting as the disturbance decoupling phytoplankton growth and mortality rates. Conversely, the processes at work during the recovery phase as described in the DRH (light-driven increases in μ, predator-prey recoupling, and eventually grazing in excess of growth) are largely mediated by the shoaling of the mixed layer. Thus although our results do not contradict the positive accumulation rates predicted by the DRH for the early stages of the recovery phase at which we sampled, the DRH implies an inverse relationship between MLD and grazing pressure that our results do not support. Although two instances at S2 when phytoplankton grazing-mortality exceeded growth may suggest that overgrazing was mediated by stratification, in all our other measurements, phytoplankton growth exceeded grazing rates regardless of MLD. In fact some of the highest grazing rates were measured where MLD was large, suggesting MLD to be a poor predictor of grazing magnitude.

Noteworthy is the linearity of the relationship between phytoplankton growth and grazing-mortality rates across the range of rates measured. This relationship corresponded to a protistan grazing impact on PP of 64%, which remarkably agrees with the estimated average for oceanic temperate/subpolar regions (Calbet and Landry 2004). The relative consistency of losses of primary production (PP) to HP grazing we observed suggests that g might be predictable if μ is known, and that the regression coefficient of 0.64 obtained in this study may serve as a useful parameter in North Atlantic carbon models.

Grazing rates were in general within the range of rates measured in previous studies conducted at similar latitudes of the North-Atlantic at different times of year in mixed layers varying between 20 m and 65 m among studies (Table 4). Our experiments yielded rates that varied from 0 d^{-1} to 0.6 d^{-1} whereas overall, previous estimates of grazing rates in the region varied from 0 d^{-1} to 1.5 d^{-1}, a broader range mostly due to one study performed in June within an eddy at 60°N, which was the only one that measured grazing rates that were on average > 1 d^{-1} (Stelfox-Widdicombe et al. 2000). Among the studies that performed multiple dilution experiments, including ours, grazing rates were variable even when mixed-layer conditions were not, thus grazing rate magnitude appeared independent of MLD, which indicates the influence of other factors.

Phytoplankton growth rates were similarly independent of MLD. We often measured phytoplankton growth rates equivalent to doubling times of 1–2 d, even in deep mixed layer conditions. At S1, our estimates of μ support previous reports of increases in phytoplankton biomass prior to stratification (Townsend et al. 1992, 1994 and ref. therein; Dale et al. 1999; Boss and Behrenfeld 2010). Surface increases in Chl *a* recorded in CTD profiles substantiated the active growth of phytoplankton suggested by our growth rate estimates.

The hypothesis that deep mixing reduces phytoplankton growth (Sverdrup 1953) and grazing-mortality (Behrenfeld 2010, 2014) relies on an essential assumption: that plankton have a homogeneous vertical distribution within the mixed layer, implying thorough mixing. Although this is a

reasonable assumption for times when the ML is consistently deepening, for this study, it was evident from the shipboard fluorescence profiles that the vertical distribution of at least the phytoplankton component was heterogeneous. The discrepancy in vertical homogeneity between the physical and chemical properties of the water column and its biological components has been pointed out by Ryther and Hulbert (1960), who observed that while nutrients, temperature, and salinity were homogeneously distributed down to 100 m, indicating thorough mixing, there was a distinct structure to the vertical distribution of phytoplankton species. Similarly, Backhaus et al. (2003) reported late winter profiles from the Iceland Basin that showed a physically homogeneous water column indicating a large MLD, but the Chl *a* profiles were heterogeneous, which the authors attributed to production enabled by convective transport of phytoplankton cells to the surface. The surface accumulations of phytoplankton biomass observed in CTD profiles from S1 also support hypotheses that surface phytoplankton biomass can increase prior to stratification if turbulence falls below some critical level (Huisman et al. 1999), which can happen even when a hydrographically defined MLD fails to reflect the depth of such turbulence (Franks, in press). At high latitudes where winter convection occurs, even a rapid, temporary switch in net heat flux across the ocean surface can give rise to shallow, quiet surface layers where phytoplankton can accumulate (Taylor and Ferrari 2011; Ferrari et al., in press; Franks, in press).

A heterogeneous distribution of phytoplankton biomass could result in aggregation of herbivorous protists (Menden-Deuer and Grünbaum 2006; Menden-Deuer 2008) and subsequent increases in grazing rates within phytoplankton patches (Menden-Deuer and Fredrickson 2010). Such uneven distribution of phytoplankton biomass as well as the ability of predators to find prey patches would indicate that mechanisms of "recoupling" (sensu Behrenfeld 2010) exist that do not require MLD to carry a stratification signature.

Franks (in press) recently argued that Sverdrup's hypothesis cannot be properly tested using estimates of MLD based on a temperature or density gradient because such estimates fail to reflect the actual intensity of in situ turbulence driving phytoplankton movement. Similarly, the effect of "dilution-recoupling" on the μ to g balance is difficult to assess in the absence of in situ measurements of turbulence, which no arbitrary criterion of temperature or density can resolve. For example, if we estimates MLD based on a potential-T threshold of $-0.1°C$ instead of $-0.2°C$—a criterion that can be used to estimate the depth of the mixing layer (de Boyer Montegut et al. 2004)—the average MLD at S1 is reduced by approx. 200 m, yet it is still vastly deeper than the euphotic zone, whereas the average MLD at S2 is hardly altered (4 m shallower). Application of this more conservative estimate of MLD does not alter the conclusion that we did not observe an association of MLD with grazing mag-

nitude. It is likely that neither estimate of MLD consistently reflected the turbulent, actively mixing layer (sensu Franks, in press), preventing prediction of phytoplankton mortality rates based on a hydrologically defined MLD. Thus a proper test of the DRH may require measurements of in situ turbulence.

Interpretation of the relationship between MLD and grazing pressure is confounded by the fact that in addition to differences in MLD, there were differences in the permanence and structure of the plankton community. The correlation found between environmental conditions and plankton assemblages implies that their relative influence on grazing magnitude could not be distinguished.

At S2, the autotrophic community was dominated by pico- and nanophytoplankton, a suitable prey-size for many protistan grazers, including ciliates (Hansen et al. 1994), which consistently dominated the enumerated HP assemblage. The MDS analysis showed little variation of the HP community over time. This stability in community composition could be a consequence of eddy formation, the likely stratification mechanism at S2. Mesoscale variabilities are frequent in the North Atlantic (Mahadevan et al. 2012) and the Norwegian Sea (Hansen et al. 2010), and satellite images showed that they were occurring in the region at the time of sampling (M. St. John pers. comm.). Eddies bar the exchange between their cores and the surrounding waters, and can trap plankton for long periods of time (Bracco et al. 2000). Stelfox-Widdicombe et al. (2000) provided evidence that an HP assemblage repeatedly sampled within an eddy remained stable even following disruption by a storm. Thus the isolating effect of an eddy could have retained a stable plankton assemblage that promoted the development of a predator population that was well matched to and able to feed on the resident prey field, resulting in the less variable grazing rates observed.

In contrast, high variability of the physical environment at S1 may have produced a frequent reconfiguration of the HP assemblage, which the MDS analysis corroborates, leading to a variable grazing response reflected in the wide variability of grazing rates. Persistence of plankton community composition and cohesion likely played an additional role in both the magnitude of g and its association with MLD.

An intriguing finding of our study is the difference in how well or poorly variations in measured Chl *a* could be reconstructed from rate estimates at the different stations. We are mindful of the limitations of comparing observed rates of change in in situ Chl *a* with the balance between experimental estimates of μ and g. Experimental constraints prevent replication of all factors potentially affecting in situ Chl *a*. This includes herbivory by copepods, a factor not assessed in our study, and our sampling frequency, which obviously produced gaps in the data. A Eularian sampling platform prevents tracking of coherent water masses (Aksnes et al. 1997; Landry et al. 2009). For example, advection may

have contributed to the overnight doubling in Chl a measured on 11 April at S1, as well as to the general variability of the rates measured there, which was greater than at the stratified site. Alternatively, undetected short-term mixing-layer shoaling could have contributed to the increase in Chl a.

An important factor that may have influenced our ability to reconstruct variations of in situ Chl a from the rate measurements is the accuracy of growth rate estimates. By maintaining phytoplankton cells at fixed irradiance levels, deck incubations undoubtedly cause an alteration of in situ light conditions, which can lead to erroneous estimates of μ (Ross et al. 2011). The error may be particularly large when deep mixing occurs, resulting in incubation light in excess of the average in situ irradiance to which deeply mixed cells are exposed, and thus in overestimates of μ. If in fact phytoplankton cells at S1 were mixed throughout the ML, we would have overestimated μ, and thus the balance between true measures of μ and estimated g may have better reflected variations of in situ Chl a. We do not believe that μ was overestimated here. Even if nonphotochemical quenching may have influenced the presence of F-max (Falkowski and Raven 2007), subsurface gradients in Chl a concentration existed at S1 that suggest vertical mixing was insufficient to eradicate them. Therefore phytoplankton distribution was vertically restricted, and thus not exposed to the range of light intensities over the entire mixed layer. Rather for at least a few hours, and in the case of repeat measurements of Chl a gradients in subsequent casts at the same station, for many hours, cells experienced the depth-specific light intensity and spectrum. Furthermore, in the case incubation light exceeded in situ irradiance, any potential intracellular decrease in Chl a as a result of photoacclimation (Ross et al. 2011) would lower growth rates estimated from changes in Chl a. Assuming the likely restricted in situ mixing of phytoplankton and given the support for active phytoplankton growth in consecutive CTD profiles, in situ irradiance variations were likely quite low and absolute incubation irradiance of subsurface water achieved using mesh screen was likely similar to in situ light conditions. Consequently, the error associated with growth rate estimates is much lower than would have been if phytoplankton were actively mixed throughout the water column.

Comparing the different stations, our results suggest that different processes controlled variations of in situ phytoplankton biomass at each oceanic station. The good agreement we found at the stratified site between in situ and rate-inferred changes in Chl a concentration would indicate that phytoplankton losses due to sinking were limited in comparison to grazing mortality. Low levels of sinking would be characteristic of the pico- and nano-size species that dominated the phytoplankton community. Diatoms, which are associated with higher sinking losses (Smayda 1970; Sarthou et al. 2005), were rare. Assuming little advection, the equiva-lence in the magnitude of estimates-inferred and in situ accumulation rates suggest that grazing mortality became the major determinant of phytoplankton biomass fluctuations.

In contrast, where the mixed layer was deep, increases in Chl a below the euphotic zone, at depths where phytoplankton growth cannot be sustained, suggested that some biomass accumulated at the surface was being vertically redistributed, explaining the majority of the mismatches between in situ changes in Chl a and those inferred by the balance between μ and g. A downward flux of phytoplankton could have been induced by episodes of shoaling allowing growth, followed by ML deepening events. There is ample literature supporting the view that the shoaling of the mixed layer is not a smooth transition but that convective mixing can vary on a daily basis, and that shoaling can be interrupted by weather-related mixing events (e.g., Brainerd and Gregg 1995; Waniek 2003; Franks, in press). Furthermore the process of mixing-induced down flux of PP is known to occur in the North Atlantic, especially early in the productive season prior to the bloom climax (Ho and Marra 1994; Backhaus et al. 2003; Waniek 2003), when episodic deepening of the mixed layer still occurs. As the mixed layer restratifies, some of the down-mixed phytoplankton inevitably becomes trapped below the thermocline and lost from the mixed layer (Backaus et al. 2003; Behrenfeld et al. 2013) and contributes to the annual carbon export of the North Atlantic (Ho and Marra 1994; Alkire et al. 2012). The different dominant loss factor at the two oceanic stations suggested by our results may imply that longer periods of stratification expected from ocean warming (Boyd and Doney 2002; Sarmiento et al. 2004) could alter the fate of biogenic carbon by reducing its export due to deep mixing before stratification and the spring bloom climax, whereas more PP could be lost to respiration associated with HP grazing.

In summary, by quantifying early spring HP grazing in the subpolar North Atlantic, we found that phytoplankton growth largely exceeded protistan grazing rates, which implies little control by predation on the potential of phytoplankton biomass to accumulate. To our knowledge this is the first measurement of predation impact on the balance of growth to predator-induced mortality losses for phytoplankton prior to the North Atlantic spring bloom biomass maximum. Given the inherent variability of marine ecosystem dynamics, a larger data set is required to verify that the stability vs. mixing mechanisms suggested here can be broadly applied. Our study highlights the importance of understanding in situ irradiance and controlling light exposure in shipboard incubations, as well as identifying vertical transport of phytoplankton as a function of MLD. Nonetheless, our data suggest that for the subpolar North Atlantic, g may be inferred from measurements of μ using a coefficient of 0.64. Furthermore, our results indicate that community composition may be an important driver of the degree to which

grazing influences phytoplankton biomass accumulation rates. Finally, the lack of association between MLD and grazing pressure found in this study cautions against predicting the effect of grazing on accumulation rates of phytoplankton biomass solely based on MLD.

References

Alkire, M. B., and others. 2012. Estimates of net community production and export using high-resolution Lagrangian measurements of O_2, NO_3^-, and POC through the evolution of a spring diatom bloom in the North Atlantic. Deep-Sea Res. I **64**: 157–174. doi:10.1016/j.dsr.2012.01.012

Aksnes, D. L., C. B. Miller, M. D. Ohman, and S. N. Wood. 1997. Estimation techniques used in studies of copepod population dynamics—a review of underlying assumptions. Sarsia **82**: 279–296. doi:10.1080/00364827.1997.10413657

Backhaus, J. O., E. Nøst Hegseth, H. Wehde, X. Irigoien, K. Hattern, and K. Logemann 2003. Convection and primary production in winter. Mar. Ecol. Prog. Ser. **251**: 1–14. doi:10.3354/meps251001

Banse, K. 1994. Grazing and zooplankton production as key controls of phytoplankton production in the open ocean. Oceanography **7**: 13–20. doi:10.5670/oceanog.1994.10

Behrenfeld, M. J. 2010. Abandoning Sverdrup's critical depth hypothesis on phytoplankton blooms. Ecology **91**: 977–989. doi:10.1890/09-1207.1

Behrenfeld, M. J. 2014. Climate-mediated dance of the plankton. Nat. Clim. Chang. **4**: 880–887. doi:10.1038/NCLIMATE2349

Behrenfeld, M. J., and E. S. Boss. 2014. Resurrecting the ecological underpinnings of ocean plankton blooms. Annu. Rev. Mar. Sci. **6**: 167–194. doi:10.1146/annurev-marine-052913-021325.

Behrenfeld, M. J., S. C. Doney, I. Lima, E. S. Boss, and D. A. Siegel. 2013. Annual cycles of ecological disturbance and recovery underlying the subarctic Atlantic spring plankton bloom. Global Biogeochem. Cycles **27**: 526–540. doi:10.1002/gbc.20050

Boss, E., and M. J. Behrenfeld. 2010. In situ evaluation of the initiation of the North Atlantic phytoplankton bloom. Geophys. Res. Lett. **37**: L18603. doi:10.1029/2010GL044174

Boyd, P., and S. C. Doney. 2002. Modelling regional responses by marine pelagic ecosystems to global climate change. Geophys. Res. Lett. **29**: 53-1-53-4. doi:10.1029/2001GL014130

Bracco, A., A. Provenzale, and I. Scheuring. 2000. Mesoscale vortices and the paradox of the plankton. Proc. R. Soc. Lond. B **267**: 1795–1800. doi:10.1098/rspb.2000.1212

Brainerd, K. E., and M. C. Gregg. 1995. Surface mixed and mixing layer depths. Deep-Sea Res. I **42**: 1521–1543. doi:10.1016/0967-0637(95)00068-H

Brody, S. R., M. S. Lozier, and J. P. Dunne. 2013. A comparison of methods to determine phytoplankton bloom initiation. J. Geophys. Res. Oceans **118**: 2345–2357. doi:10.1002/jgrc.20167

Brussaard, C. 2004. Viral control of phytoplankton populations—a review. J. Eukaryot. Microbiol. **51**: 125–138. doi:10.1111/j.1550-7408.2004.tb00537.x

Burkill, P. H., E. S. Edwards, A. W. G. John, and M. A. Sleigh. 1993. Microzooplankton and their herbivorous activity in the northeastern Atlantic Ocean. Deep-Sea Res. II **40**: 479–493. doi:10.1016/0967-0645(93)90028-L

Calbet, A., and M. R. Landry. 2004. Phytoplankton growth, microzooplankton grazing, and carbon cycling in marine systems. Limnol. Oceanogr. **49**: 51–57. doi:10.4319/lo.2004.49.1.0051

Caron, D. A., M. R. Dennett, D. J. Lonsdale, D. M. Moran, and L. Shalapyonok. 2000. Microzooplankton herbivory in the Ross Sea, Antarctica. Deep-Sea Res. II **47**: 3249–3272. doi:10.1016/S0967-0645(00)00067-9

Clarke, K. R. 1993. Non-parametric multivariate analyses of changes in community structure. Aust. J. Ecol. **18**: 117–143. doi:10.1111/j.1442-9993.1993.tb00438.x

Clarke, K. R., and R. N. Gorley. 2006. PRIMER v6: User Manual/Tutorial. PRIMER-E, Plymouth.

Clarke, K. R., and R. M. Warwick. 2001. A further biodiversity index applicable to species lists: Variation in taxonomic distinctness. Mar. Ecol. Prog. Ser. **216**: 265–278. doi:10.3354/meps216265

Dale, T., F. Rey, and B. R. Heimdal. 1999. Seasonal development of phytoplankton at a high latitude oceanic site. Sarsia **84**: 419–435. doi:10.1080/00364827.1999.10807347

Davis, P. G., and J. M. Sieburth. 1982. Differentiation of phototrophic and heterotrophic nanoplankton populations in marine waters by epifluorescence microscopy. Ann. Inst. Oceanogr. **58**: 249–260.

de Boyer Montégut, C., G. Madec, A. S. Fischer, A. Lazar, and D. Iudicone. 2004. Mixed layer depth over the global ocean: An examination of profile data and a profile-based climatology. J. Geophys. Res. **109**: C12003. doi:10.1029/2004JC002378

Dodge, J. D. 1982. Marine dinoflagellates of the British Isles. Her Majesty's Stationery Office.

Falkowski, P. G., and J. A. Raven. 2007. Aquatic photosynthesis, 2nd ed. Princeton Univ. Press.

Ferrari, R., S. T. Merrifield, and J. R. Taylor. In press. Shutdown of convection triggers increase of surface chlorophyll. J. Mar. Syst. doi:10.1016/j.jmarsys.2014.02.009

Flynn, K. J., and others. 2013. Misuse of the phytoplankton-zooplankton dichotomy: The need to assign organisms as mixotrophs within plankton functional types. J. Plankton Res. **35**: 3–11. doi:10.1093/plankt/fbs062

Franks, P. J. S. In press. Has Sverdrup's critical depth hypothesis been tested? Mixed layers vs. turbulent layers. ICES J. Mar. Sci. doi:10.1093/icesjms/fsu175

Gaul, W., and A. N. Antia. 2001. Taxon-specific growth and selective microzooplankton grazing of phytoplankton in the Northeast Atlantic. J. Mar. Syst. **30**: 241–261. doi: 10.1016/S0924-7963(01)00061-6

Gifford, D. J., L. M. Fessenden, P. R. Garrahan, and E. Martin. 1995. Grazing by microzooplankton and meso-zooplankton in the high-latitude North Atlantic Ocean: Spring versus summer dynamics. J. Geophys. Res. **100**: 6665–6675. doi:10.1029/94JC00983

Gran, H. H., and T. Braarud. 1935. A quantitative study on the phytoplankton of the Bay of Fundy and the Gulf of Maine (including observations on hydrography, chemistry and morbidity). J. Biol. Board Can. **1**: 279–467. doi: 10.1139/f35-012

Graff, J. R., and T. A. Rynearson. 2011. Extraction method influences the recovery of phytoplankton pigments from natural assemblages. Limnol. Oceanogr.: Methods **9**: 129–139. doi:10.4319/lom.2011.9.129

Hansen, B., P. K. Bjornsen, and P. J. Hansen. 1994. The size ratio between planktonic predators and their prey. Limnol. Oceanogr. **39**: 395–403. doi:10.4319/lo.1994.39.2.0395

Hansen, C., E. Kvaleberg, and A. Samuelsen. 2010. Anticyclonic eddies in the Norwegian Sea; their generation, evolution and impact on primary production. Deep-Sea Res. I **57**: 1079–1091. doi:10.1016/j.dsr.2010.05.013

Hansen, P. J., M. Moldrup, W. Tarangkoon, L. Garcia-Cuetos, and Ø. Moestrup. 2012. Direct evidence for symbiont sequestration in the marine red tide ciliate *Mesodinium rubrum*. Aquat. Microb. Ecol. **66**: 63–75. doi:10.3354/ame01559

Henson, S. A., I. Robinson, J. T. Allen, and J. Waniek. 2006. Effect of meteorological conditions on interannual variability in timing and magnitude of the spring bloom in the Irminger Basin, North Atlantic. Deep-Sea Res. I **53**: 1601–1615. doi:10.1016/j.dsr.2006.07.009

Ho, C., and J. Marra. 1994. Early-spring export of phytoplankton production in the northeast Atlantic Ocean. Mar. Ecol. Prog. Ser. **114**: 197–202. doi:10.3354/meps114197

Huisman, J., M. Arrayás, U. Ebert, and B. Sommeijer. 2002. How do sinking phytoplankton species manage to persist? Am. Nat. **159**: 245–254. doi:10.1086/338511

Huisman, J., P. van Oostveen, and F. J. Weissing. 1999. Critical depth and critical turbulence: Two different mechanisms for the development of phytoplankton blooms. Limnol. Oceanogr. **44**: 1781–87. doi:10.4319/lo.1999.44.7.1781

Irigoien, X., K. J. Flynn, and R. P. Harris. 2005. Phytoplankton blooms: A 'loophole' in microzooplankton grazing impact? J. Plankton Res. **27**: 313–321. doi:10.1093/plankt/fbi011

Jespersen, A. M., and K. Christoffersen. 1987. Measurements of chlorophyll-a from phytoplankton using ethanol as extraction solvent. Arch. Hydrobiol. **109**: 445–454.

Kraberg, A., M. Baumann, and C.-D. Dürselen. 2010. Coastal phytoplankton: photo guide for Northern European Seas. Verlag Dr. Friedrich Pfeil.

Landry, M. R., and R. P. Hassett. 1982. Estimating the grazing impact of marine microzooplankton. Mar. Biol. **67**: 283–288. doi:10.1007/BF00397668

Landry, M. R., M. D. Ohman, R. Goericke, M. R. Stukel, and K. Tsyrklevich. 2009. Lagrangian studies of phytoplankton growth and grazing relationships in a coastal upwelling ecosystem off Southern California. Prog. Oceanogr. **83**: 208–216. doi:10.1016/j.pocean.2009.07.026

Lawrence, C., and S. Menden-Deuer. 2012. Drivers of protistan grazing pressure: Seasonal signals of plankton community composition and environmental conditions. Mar. Ecol. Prog. Ser. **459**: 39–52. doi:10.3354/meps09771

Lindemann, C., and M. A. St. John. 2014. A seasonal diary of phytoplankton in the North Atlantic. Front. Mar. Sci. **1**: 1–6. doi: 10.3389/fmars.2014.00037

Mahadevan, A., E. D'Asaro, C. Lee, and M. J. Perry. 2012. Eddy-driven stratification initiates North Atlantic spring phytoplankton blooms. Science **337**: 54–58. doi:10.1126/science.1218740

Martin, P., R. S. Lampitt, M. J. Perry, R. Sanders, C. Lee, and E. D'Asaro. 2011. Export and mesopelagic particle flux during a North Atlantic spring diatom bloom. Deep-Sea Res. I **58**: 338–349. doi:10.1016/j.dsr.2011.01.006

Menden-Deuer, S. 2008. Spatial and temporal characteristics of plankton-rich layers in a shallow, temperate fjord. Mar. Ecol. Prog. Ser. **355**: 21–30. doi:10.3354/meps07265

Menden-Deuer, S., and K. Fredrickson. 2010. Structure-dependent protistan grazing and its implication for the formation, maintenance and decline of plankton patches. Mar. Ecol. Prog. Ser. **420**: 57–71. doi:10.3354/meps08855

Menden-Deuer, S., and D. Grünbaum. 2006. Individual foraging behaviors and population distributions of a planktonic predator aggregating to phytoplankton thin layers. Limnol. Oceanogr. **51**: 109–116. doi:10.4319/lo.2006.51.1.0109

Menden-Deuer, S., and E. J. Lessard. 2000. Carbon to volume relationships for dinoflagellates, diatoms, and other protist plankton. Limnol. Oceanogr. **45**: 569–579. doi: 10.4319/lo.2000.45.3.0569

Menden-Deuer, S., E. J. Lessard, and J. Satterberg. 2001. Effect of preservation on dinoflagellate and diatom cell volume and consequences for carbon biomass predictions. Mar. Ecol. Prog. Ser. **222**: 41–50. doi:10.3354/meps222041

Montagnes, D. J. S., and D. H. Lynn. 1991. Taxonomy of Choreotrichs, the major marine planktonic ciliates, with emphasis on the aloricate forms. Mar. Microb. Food Webs **5**: 59–74.

Putt, M., and D. K. Stoecker. 1989. An experimentally determined carbon:volume ratio for marine "oligotrichous" ciliates from estuarine and coastal waters. Limnol. Oceanogr. **34**: 1097–1103. doi:10.4319/lo.1989.34.6.1097

Rose, J. M., and D. A. Caron. 2007. Does low temperature constrain the growth rates of heterotrophic protists? Evidence and implications for algal blooms in cold waters. Limnol. Oceanogr. **53**: 886–895. doi:10.4319/lo.2007.52.2.0886

Ross, O. N., R. J. Geider, E. Berdalet, M. L. Artigas, and J. Piera. 2011. Modeling the effect of vertical mixing on bottle incubations for determining in situ phytoplankton dynamics. I. Growth rates. Mar. Ecol. Prog. Ser. **435**: 13–31. doi:10.3354/meps09193

Ryther, J. H., and E. M. Hulburt. 1960. On winter mixing and the vertical distribution of phytoplankton. Limnol. Oceanogr. **5**: 337–338. doi:10.4319/lo.1960.5.3.0337

Sarmiento, J. L., and others. 2004. Response of ocean ecosystems to climate warming. Global Biogeochem. Cycles **18**: GB3003. doi:10.1029/2003GB002134

Sarthou, G., K. R. Timmermans, S. Blain, and P. Treguer. 2005. Growth physiology and fate of diatoms in the ocean: a review. J. Sea Res. **53**: 25–42. doi:10.1016/j.seares.2004.01.007

Sherr, E. B., and B. F. Sherr. 2002. Significance of predation by protists in aquatic microbial food webs. A. Van Leeuw. **81**: 293–308. doi:10.1023/A:1020591307260

Sherr, E. B., and B. F. Sherr. 2009. Capacity of herbivorous protists to control initiation and development of mass phytoplankton blooms. Aquat. Microb. Ecol. **57**: 253–262. doi:10.3354/ame01358

Sherr, E. B., B. F. Sherr, and C. Ross. 2013. Microzooplankton grazing impact in the Bering Sea during spring sea ice conditions. Deep-Sea Res. II **94**: 57–67. doi:10.1016/j.dsr2.2013.03.019

Sherr, E. B., B. F. Sherr, P. A. Wheeler, and K. Thompson. 2003. Temporal and spatial variation in stocks of autotrophic and heterotrophic microbes in the upper water column of the central Arctic Ocean. Deep-Sea Res. I **50**: 557–571. doi:10.1016/S0967-0637(03)00031-1

Siegel, D. A., S. C. Doney, and J. A. Yoder. 2002. The North Atlantic spring phytoplankton bloom and Sverdrup's critical depth hypothesis. Science **296**: 730–733. doi:10.1126/science.1069174

Smayda, T. J. 1970. The suspension and sinking of phytoplankton in the Sea. Oceanogr. Mar. Biol. Ann. Rev. **8**: 353–414.

Smayda, T. J. 1997. What is a bloom? A commentary. Limnol. Oceanogr. **42**: 1132–1136. doi:10.4319/lo.1997.42.5_part_2.1132

Smetacek, V. S. 1981. The annual cycle of protozooplankton in the Kiel Bight. Mar. Biol. **63**: 1–11. doi:10.1007/BF00394657

Smith, W. O., and E. Sakshaug. 1990. Polar phytoplankton, p. 477–525. In W. O. Smith [ed.]. Polar Oceanography, Part B. Academic Press.

Stelfox-Widdicombe, C. E., E. S. Edwards, P. H. Burkill, and M. A. Sleigh. 2000. Microzooplankton grazing activity in the temperate and sub-tropical NE Atlantic: Summer 1996. Mar. Ecol. Prog. Ser. **208**: 1–12. doi:10.3354/meps208001

Strom, S. L., and K. A. Fredrickson. 2008. Intense stratification leads to phytoplankton nutrient limitation and reduced microzooplankton grazing in the southeastern Bering Sea. Deep-Sea Res. II **55**: 1761−1774. doi:10.1016/j.dsr2.2008.04.008

Strüder-Kypke, M. C., E. R. Kypke, S. Agatha, J. Warwick, and D. J. S. Montagnes. 2002. The user-friendly guide to coastal planktonic ciliate. Available from http://www.zooplankton.cn/Default.aspx?tabid=604andlanguage=zh-CN.

Sverdrup, H. U. 1953. On conditions of the vernal blooming of phytoplankton. J. Conseil **18**: 287–295. doi:10.1093/icesjms/18.3.287

Takahashi, T., and others. 2009. Climatological mean and decadal change in surface ocean pCO$_2$ and net sea–air CO$_2$ flux over the global oceans. Deep-Sea Res. II **56**: 554–577. doi:10.1016/j.dsr2.2008.12.009

Taylor, A. H., D. S. Harbour, R. P. Harris, P. H. Burkill, and E. S. Edwards. 1993. Seasonal succession in the pelagic ecosystem of the North Atlantic and the utilization of nitrogen. J. Plankton Res. **15**: 875–891. doi:10.1093/plankt/15.8.875

Taylor, J. R., and R. Ferrari. 2011. Shutdown of turbulent convection as a new criterion for the onset of spring phytoplankton blooms. Limnol. Oceanogr. **56**: 2293–2307. doi:10.4319/lo.2011.56.6.2293

Throndsen, J., G. R. Hasle, and K. Tangen. 2007. Phytoplankton of Norwegian coastal waters. Almater Forlag As.

Townsend, D. W., L. M. Cammen, P. M. Holligan, D. E. Campbell, and N. R. Pettigrew.1994. Causes and consequences of variability in the timing of spring phytoplankton blooms. Deep-Sea Res. I **4**: 747–765. doi:10.1016/0967-0637(94)90075-2

Townsend, D. W., M. D. Keller, M. E. Sieracki, and S. G. Ackleson. 1992. Spring phytoplankton blooms in the absence of vertical water column stratification. Nature **360**: 59–62. doi:10.1038/360059a0

Turner, J. T. 2002. Zooplankton fecal pellets, marine snow and sinking phytoplankton blooms. Aquat. Microb. Ecol. **27**: 57–102. doi:10.3354/ame027057

Utermöhl, H. 1958. Zur Vervollkommnung der quantitativen Phytoplankton-Methodik. Internationale Verereinigung für Theoretische und Angewandte Limnologie: Mitteilungen **9**: 1−38.

Verity, P. G., and C. Langdon. 1984. Relationships between lorica volume, carbon, nitrogen, and ATP content of tintinnids in Narragansett Bay. J. Plankton Res. **6**: 859–868. doi:10.1093/plankt/6.5.859

Verity, P. G., P. Wassmann, T. N. Ratkova, I. J. Andreassen, and E. Nordby. 1999. Seasonal patterns in composition and biomass of autotrophic and heterotrophic nano- and microplankton communities on the north Norwegian shelf. Sarsia **84**: 265–277. doi:10.1080/00364827.1999.10420431

Waniek, J. J. 2003. The role of physical forcing in initiation of spring blooms in the northeast Atlantic. J. Mar. Sys. **39**: 57–82. doi:10.1016/S0924-7963(02)00248-8

Wolfe, G. V., M. Levasseur, G. Cantin, and S. Michaud. 2000. DMSP and DMS dynamics and microzooplankton grazing in the Labrador Sea: Application of the dilution technique. Deep-Sea Res. I **47**: 2243–2264. doi:10.1016/S0967-0637(00)00028-5

Worden, A. Z., and B. J. Binder. 2003. Application of dilution experiments for measuring growth and mortality rates among *Prochlorococcus* and *Synechococcus* populations in oligotrophic environments. Aquat. Microb. Ecol. **30**: 159–174. doi:10.3354/ame030159

Zar, J. H. 2010. Biostatistical analysis, 5th ed. Pearson Prentice-Hall.